Seismic Response Characteristics of Complex Slope Terrain Based on FLAC3D Numerical Simulation

Jiale Yang [1, *], Yongchao Jiang [2]

[1] School of Materials and Civil Engineering, Jiangsu University Jingjiang College, Zhenjiang, China, 212028

[2] School of Mechanics and Civil Engineering, China University of Mining & Technology, Beijing, Beijing, China, 102206

* Corresponding Author Email: 17712847548@163.com

Abstract. In the southwestern region of China, there are many natural slopes due to various factors such as terrain and landforms. Additionally, a large number of engineering projects are constructed in this region. When constructing highways, it is inevitable to build numerous cut slopes. Unfortunately, the seismic belt of China is mainly distributed in the southwestern region. Therefore, studying the dynamic response of cut slopes under seismic excitation is particularly important to reduce the occurrence of natural disasters such as landslides. This study utilizes numerical simulation methods to investigate the stability of different cut slopes. The results indicate that the acceleration dynamic response and displacement dynamic response exhibit elevation amplification effects. In the case of stepped cut slopes, the acceleration on the outer side of the steps is greater than that on the inner side, and the displacement on the outer side is larger as well. Additionally, the stress on the outer side is smaller compared to the inner side. As the platform width increases, the acceleration on the outer side decreases while the inner side accelerates. Similarly, the displacement on the outer side decreases while it increases on the inner side. Furthermore, the stress on the outer side increases while it decreases on the inner side. Consequently, as the slope angle of the slopes increases, the stability of the slopes deteriorates. Conversely, as the platform width increases, the stability of the slopes improves. The findings of this study can provide guidance for the construction and reinforcement of slope engineering, especially in the context of stepped slopes.

Keywords: Seismic Waves, Dynamic Response, Numerical Modelling, Elevation Amplification Effects.

1. Introduction

Catastrophic earthquakes are unpredictable and widespread, and seismic geological hazards caused by earthquake-induced slope instability and damage are serious and have attracted extensive attention from different disciplines [1]. In addition to the direct damage caused by earthquakes to buildings, the secondary geological hazards induced by earthquakes, such as landslides and avalanches, may cause even greater loss of life and property [2].

In the southwestern region of China, there are continuous mountains, deep valleys, and rugged terrain, resulting in numerous natural slopes. This region is located at the junction of the Eurasian Plate and the Indian Plate, and its geological structure is extremely complex. The complex geological structure causes stress in the Earth's crust to concentrate more easily, leading to frequent earthquakes and a large number of landslides. These natural disasters have caused significant losses to people's lives and properties. For example, on May 12, 2008, the Wenchuan earthquake in Sichuan Province, with a magnitude of 8.0, resulted in approximately 90,000 deaths and 370,000 injuries. On April 20, 2013, the Lushan earthquake in Ya'an, Sichuan Province, with a magnitude of 7.0, caused about 196 deaths and 11,000 injuries. On August 8, 2017, the Jiuzhaigou earthquake in Jiuzhaigou, Sichuan Province, with a magnitude of 7.0, resulted in approximately 25 deaths and 493 injuries. Due to the unique geographical environment, there are a large number of landslides and debris flows. For example, among the 11,407 hidden points of geological hazards in the severely affected areas of the Wenchuan earthquake, there were 4,800 landslides and 1,277 debris flow points [3]. With the implementation of China's western development and "One Belt, One Road" policy, the southwestern

region emerged in the construction of highways and railway passenger dedicated line wave, and the southwest is mostly a high-intensity seismic zone, the stability of the seismic effects of the problem is becoming more and more prominent, and the construction of highways and railway passenger dedicated line, and the construction of highways and railway passenger dedicated line[4]. Therefore, studying the dynamic stability of slopes under seismic action is of great significance in this region.

In recent years, many research achievements have been made in the study of the dynamic response characteristics and stability analysis of slopes. For example, Zhou Zehua (2023) [5] conducted research on the dynamic response and time-frequency stability of slopes with through-going structural planes. Wang Jibo (2023) [6] analyzed the three-dimensional dynamic response of hazardous slopes. Ma Chenyang (2022) [7] evaluated the dynamic response and stability of bank slopes. Tian Junyu (2022) [8] conducted numerical simulation research on the dynamic response and stability of foundation-covered accumulation slopes. Qi Shengwen et al. [9-11] analysed the dynamic response law of slopes through numerical calculations to investigate the influencing factors of slope stability under seismic action. Ye Shuaihua, et al. (2020) [12] analyzed the dynamic response characteristics and stability of multi-level high-filled slopes in loess. Huang Shiyuan, et al. (2015) [13] studied the influence of platform width on the dynamic response and stability of slopes.

However, the current analysis of seismic dynamic response characteristics and stability mainly focuses on high slopes, steep slopes, or weak slopes, and there is limited research on stepped slopes and variations in step width. In the traditional slope calculation, the influence of the step width on the stability of the slope is often ignored, and if the traditional calculation method is followed, there is a great safety risk [14]. This paper takes three different cut slopes as the background and uses the FLAC3D finite difference software to establish numerical models of the three slopes. The dynamic response characteristics and stability of the cut slopes under seismic waves are analyzed. The research results can provide certain guidance for the seismic resistance of slope engineering in the southwestern region of China.

2. Numerical model setup

2.1. Introduction of numerical software

FlAC3D, known as Fast Lagrangian Analysis of Continua, uses explicit Lagrangian algorithms and hybrid-discrete partitioning techniques to detect plastic damage and flow of simulated materials very accurately and without the need to form stiffness matrices, and solves a wide range of three-dimensional geotechnical engineering problems using a small amount of computational resources [15].

2.2. Numerical modelling and parameter setting

In this paper, three cut slopes of a highway in Southwest China were taken as the research objects, and the numerical models shown in Fig.1 and the models were established after appropriate generalization.

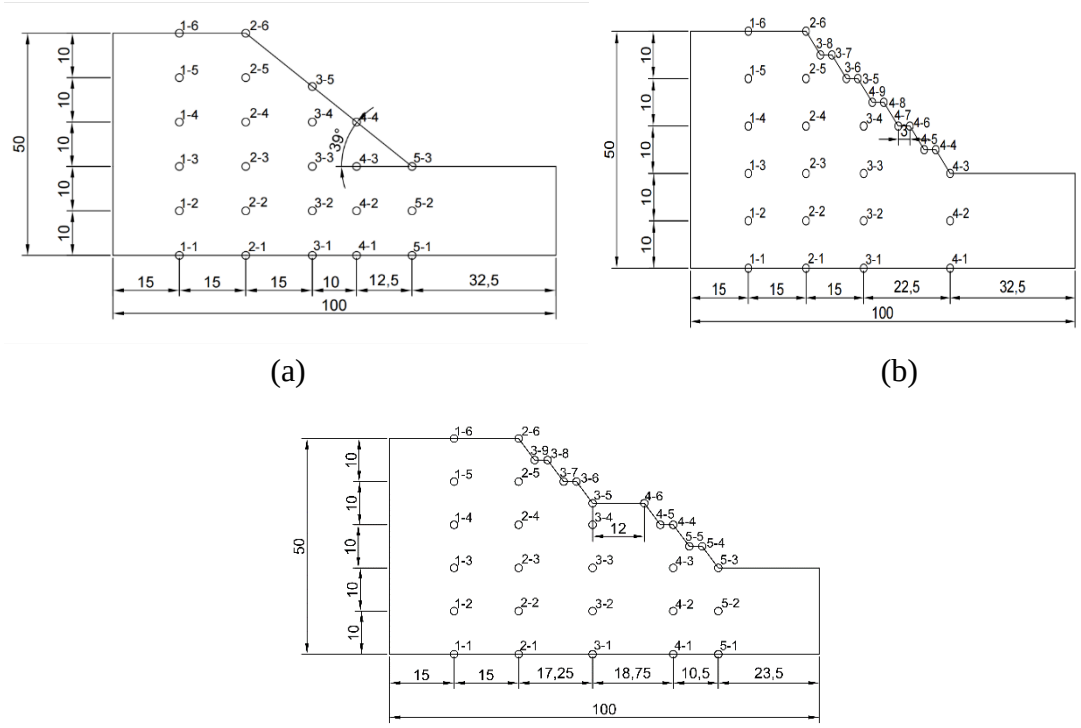

Fig. 1 Caculating model for different slopes.

In order to study the distribution patterns of acceleration, displacement, stress, and shear strain increments within the interior of slopes with different terrain under seismic actions, different monitoring points were set up for each slope.

The first model, as shown in Fig.1(a), was designed with five groups of monitoring points, numbered from 1-1 to 5-3, resulting in a total of 24 monitoring points. The second model, depicted in Fig.1(b), consisted of four groups of monitoring points, numbered from 1-1 to 4-9, totaling 29 monitoring points. The third model, illustrated in Fig.1(c), included five groups of monitoring points, numbered from 1-1 to 5-5, giving a total of 31 monitoring points.

The seismic waves used for the dynamic analysis in this study are shown in Fig.4. The waveforms were extracted from the main energy range of 0 to 40 seconds and the maximum amplitude was set at 0.4g. During the loading process, the input acceleration varied from 0.1g to 0.4g. This parameter range was chosen to investigate the distribution patterns of response acceleration, displacement, stress, and other factors within the interior of slopes with different terrain under varying input accelerations. The physical and mechanical parameters are shown in Table 1.

Table. 1 Physical and mechanical properties of slopes

Serial number	Density (kg/m^3)	Bulk (Pa)	Shear (Pa)	Cohesion (Pa)	Internal friction angle
Rock	2500	2.5e9	1.2e9	500e3	30
Rock-1	2500	2.5e9	1.2e9	500e3	30
Rock-2	2500	2.5e9	1.2e9	500e3	30

2.3. Seismic wave loading

The seismic wave selected for this dynamic analysis is shown in Fig. 2, intercepting the main energy section 0-40s as the input wave, with the highest amplitude of 0.4g. When loading, the input acceleration is loaded from 0.1g to 0.4g, respectively, to study the distribution law of the response acceleration, displacement, and stress of the different slope topography in the interior of the slope during the change of the input acceleration.

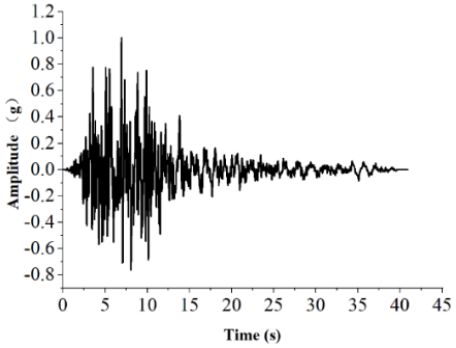

Fig. 2 The input seismic waveforms

3. Result analysis

3.1. Acceleration responses analyses

For the acceleration analysis of a single embankment slope, when the input acceleration is varied from 0.1g to 0.4g, the relationship between response acceleration and relative elevation can be obtained. The point-line graph of response acceleration relative to the elevation is plotted for monitoring points 2-1 to 2-6, as shown in Fig. 3(a). From Fig. 3(a), it can be observed that there is an elevation amplification effect on the acceleration, and as the input acceleration increases, the response acceleration also increases.

To identify the monitoring point with the maximum response acceleration, two point-line graphs of response acceleration relative to elevation are plotted for monitoring points 1-1 to 1-6 and monitoring points 3-1 to 3-5, as shown in Fig. 3(b) and Fig. 3(c) respectively. By comparing the locations of maximum response acceleration in Fig. 3(b), Fig. 3(c), and Fig. 3(a), it is determined that monitoring point 2-6 has the highest acceleration response. This is attributed to the relatively smaller constraints on the slope at the top, resulting in a larger acceleration response.

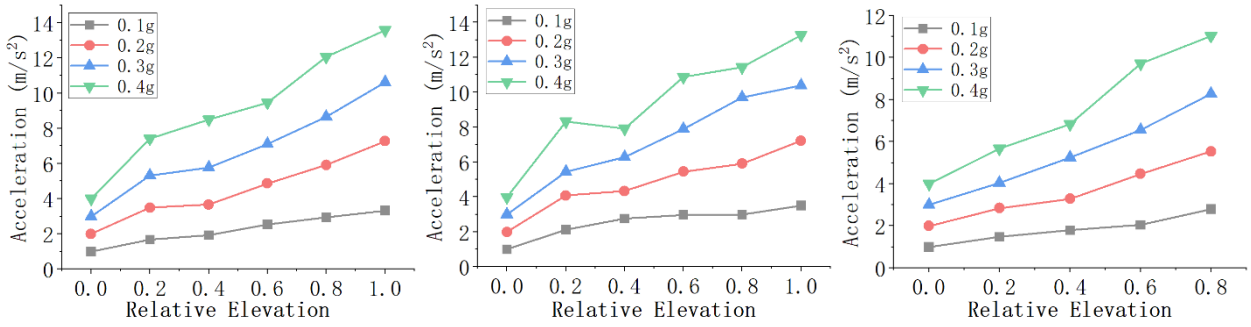

Fig. 3 (a) Monitoring Point 1-1 to Monitoring Point 1-6 (b) Monitoring Point 2-1 to Monitoring Point 2-6 (c) Monitoring Point 3-1 to Monitoring Point 3-5

For the acceleration analysis of a stepped slope, similar to a single slope embankment, the acceleration exhibits an elevation amplification effect, meaning that as the input acceleration increases, the response acceleration also increases. Monitoring point 2-6 represents the location with the maximum acceleration response. However, there is a difference between a stepped embankment slope and a single slope embankment due to the presence of steps. This difference manifests in the acceleration magnitudes at the outer and inner corners.

As shown in Fig. 4, for a stepped embankment slope, the acceleration magnitudes have a relationship between the outer and inner corners. Specifically, the acceleration at monitoring point 3-7 is greater than at monitoring point 3-8, the acceleration at monitoring point 3-5 is greater than at monitoring point 3-6, the acceleration at monitoring point 4-8 is greater than at monitoring point 4-9, the acceleration at monitoring point 4-6 is greater than at monitoring point 4-7, and the acceleration

at monitoring point 4-4 is greater than at monitoring point 4-5. Therefore, for a stepped embankment slope, the acceleration at the outer corners is greater than at the inner corners.

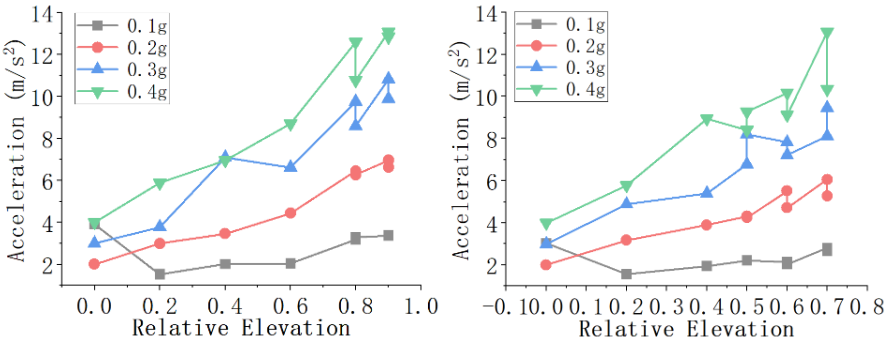

Fig. 4 Acceleration Power Response + Monitoring Points

For the acceleration analysis of a stepped embankment slope with an increased platform width, compared to a regular stepped slope, an additional passageway is added, resulting in the widening of the platform. To investigate the relationship between the accelerations at monitoring points 3-5 and 4-6 for the widened platform and monitoring points 4-8 and 4-9 for the regular stepped slope, a comparison can be made using the difference method. The peak accelerations at monitoring points 3-5, 4-6, and monitoring points 4-8, 4-9, along with the input acceleration, can be plotted on a point-line graph as shown in Fig. 5, By subtracting the values, it can be observed that with the increase in platform width, the acceleration at the outer corners decreases, while the acceleration at the inner corners increases.

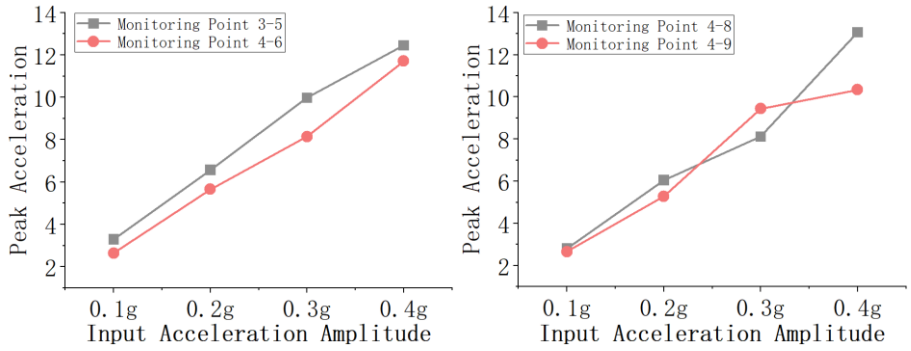

(a) (b)

Fig. 5 (a) Monitoring points 3-5 and 4-9 (b) Monitoring points 4-6 and 4-8

3.2. Displacement responses

For the displacement analysis of the slopes on a single slope, the relationship between the displacement response and the relative upper level can be obtained when the input acceleration is loaded from 0.1g to 0.4g. The point line plots of the response displacement versus relative high level from monitoring point 2-1 to monitoring point 2-6 are shown in Fig. 6(a). From Fig. 6(a), the displacement response has an elevation amplification effect and the larger the input acceleration, the larger the displacement response acceleration. In order to find the monitoring point with the largest displacement response, two point line plots of displacement response versus relative height for monitoring point 1-1 to monitoring point 1-6 and monitoring point 3-1 to monitoring point 3-5 are plotted as shown in Fig. 6(b) and Fig. 6(c), and we compare the largest point of displacement response in Fig. 6(b) and Fig. 6(c) with Fig. 6(a), and conclude that the largest displacement response is found at monitoring point 2-6, which is due to the smaller constraints on the location of the top of the slope, resulting in a larger acceleration.

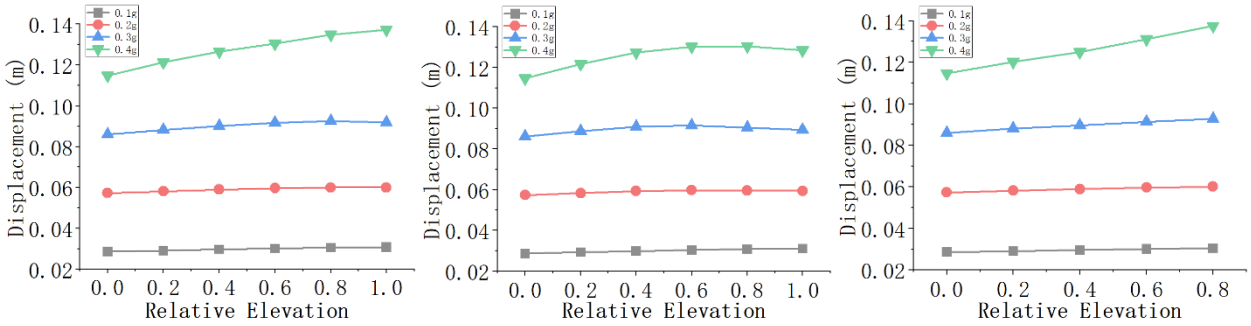

Fig. 6 (a) Monitoring point 2-1 to Monitoring point 2-6 (b) Monitoring point 1-1 to Monitoring point 1-6

(c) Monitoring point 3-1 to Monitoring point 3-5

For the analysis of displacement on the stepped slopes, it is observed that the response exhibits an elevation amplification effect. Additionally, as the input acceleration increases, the acceleration of the displacement response also increases. This behavior is similar to that observed in single slope cases. Among the monitoring points (2-6), points 2-6 exhibit the maximum displacement response. Similar to the acceleration analysis of the slopes, the displacements at the outer and inner corners of the two slopes show a proportional relationship. Specifically, when observing Fig. 7(a) and Fig. 7(b), it becomes evident that the displacement at monitoring point 3-7 is greater than the displacement at monitoring point 3-8. Similarly, the displacement at monitoring point 3-5 is larger than the displacement at point 3-6. Furthermore, the displacement at monitoring point 4-8 is greater than the displacement at monitoring point 4-9, while the displacement at monitoring point 4-6 is larger than that at point 4-7. Lastly, the displacement at monitoring point 4-4 is larger than that at monitoring point 4-5. Consequently, for the stepped rift valley slopes, the outer corners experience greater displacement compared to the inner corners.

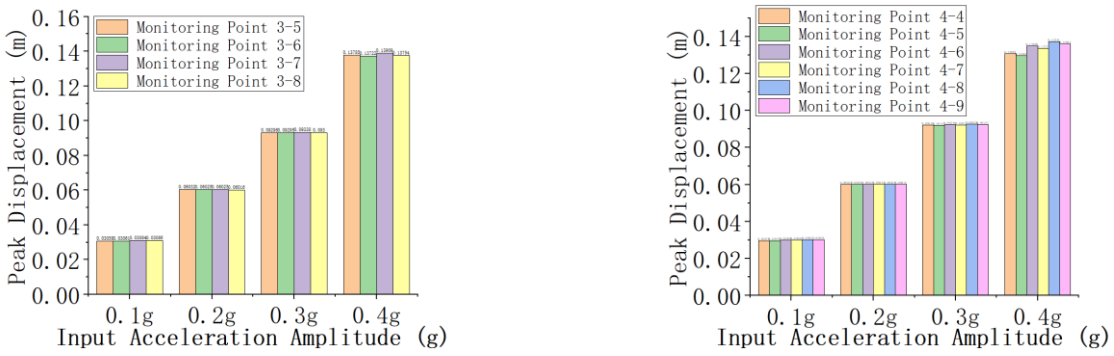

Fig. 7 (a) Monitoring points 3-5, 3-6, 3-7 and 3-8 (b) Monitoring Points 4-4, 4-5, 4-6, 4-7, 4-8 and 4-9

For the displacement analysis of roadway slopes with increased width of stepped platform, to study the relationship between the displacements of monitoring points 3-5, 4-6 and monitoring points 4-8, 4-9 of stepped slopes after the increase of platform width, the comparison can be made by making difference method. The histograms of peak displacement versus input acceleration for monitoring points 3-5, 4-6 and monitoring points 4-8, 4-9 are plotted as shown in Fig. 8(a) and Fig. 8(b), and the difference is made to obtain that with the increase of platform width, the outer corner displacement decreases, and the inner corner displacement increases.

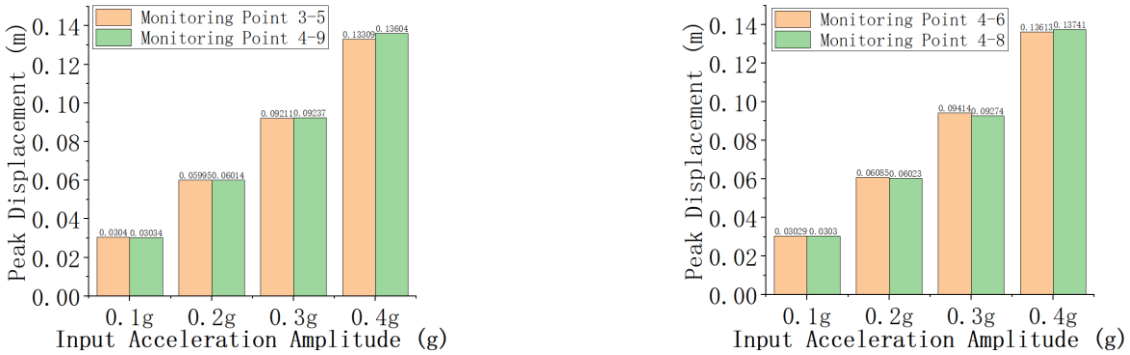

(a) (b)

Fig. 8 (a) Monitoring points 3-5 and 4-9 (b) Monitoring points 4-6 and 4-8

3.3. Stress analysis

For the stress analysis of road slopes on a single slope, the relationship between stress and relative upper level can be determined by applying input acceleration ranging from 0.1g to 0.4g. Fig. 9 illustrates a point line plot of stress versus relative high level from monitoring point 1-1 to monitoring point 1-6. Observing Fig. 9, it becomes evident that the stress distribution increases gradually from the top to the bottom. This behavior is a result of the increasing constraints imposed by the soil body, leading to an elevation-induced stress increase. To establish the relationship between peak input acceleration and elevation, input acceleration versus stress plots is depicted for the face and bottom of the slope in Fig. 10. Analyzing the graph, it can be observed that for a peak input acceleration of 0.1g, the stress rises from 6.5kPa to 232kPa over a 50m decrease in elevation from the slope face to the slope bottom, indicating an increase of 35.7 times. Similarly, for peak input accelerations of 0.2g, 0.3g, and 0.4g, the stress exhibits increase of 19.4 times, 22.59 times, and 18.6 times, respectively. As such, the stress amplification decreases as the peak input acceleration value increases. Furthermore, the stress at monitoring point 5-3 attains the highest value. This can be attributed to the fact that this point is located at the foot of the slope, where the upper soil body experiences seismic excitation and exerts pressure on the slope's base. Consequently, stress concentration occurs, posing potential risks to the stability of the slope's foot.

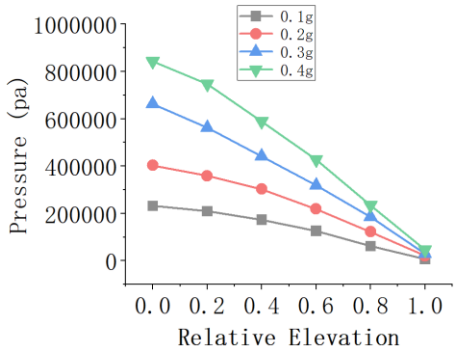

Fig. 9 Monitoring Point 1-1 to Monitoring Point 1-6 Monitoring Points

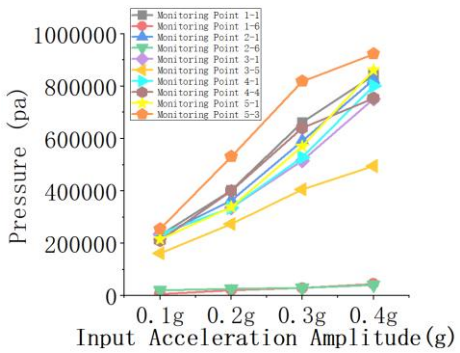

Fig. 10 Slope Face and Base

Stress analysis was conducted on terrace-type riffle slopes, and similar to single-slope riffle slopes, the stress distribution increases from top to bottom. This phenomenon is attributable to the growing constraints imposed by the soil body, resulting in elevated stress levels. To identify the monitoring point with the highest stress, a point-line diagram depicting stress versus relative elevation was plotted, as displayed in Fig. 11(a) and Fig. 11(b). From the graph, it is evident that monitoring point 4-5 exhibits the highest stress. This can be attributed to its position as the shear exit point, where the upper soil body experiences seismic excitation, leading to stress concentration and the potential for sliding at this location. Additionally, the stress relationship between the outer and inner corners of the slope can be determined. Monitoring point 3-7 experiences lower stress compared to monitoring

point 3-8, while monitoring point 3-5 has lower stress than monitoring point 3-6. Similarly, monitoring point 4-8 has lower stress than monitoring point 4-9, monitoring point 4-6 has lower stress than monitoring point 4-7, and monitoring point 4-4 has lower stress than monitoring point 4-5. Hence, for step-type road riffle slopes, the stress levels at the outer corners are lower than those at the inner corners.

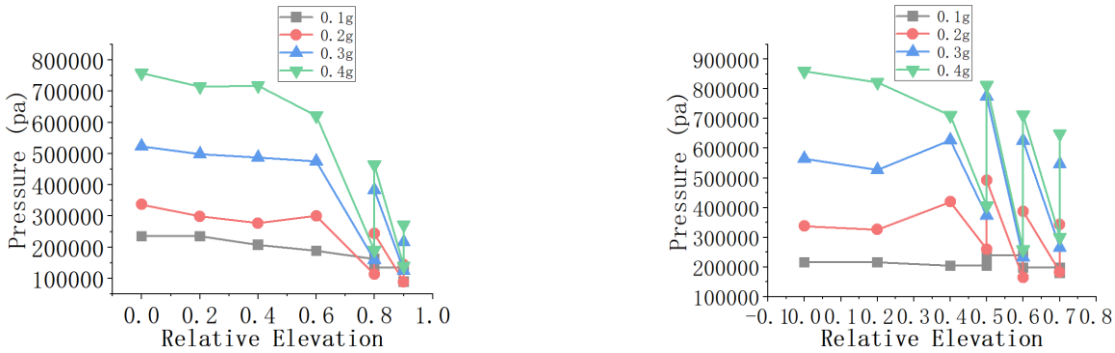

Fig. 11 (a) Monitoring Points 3-1-3-8 (b) Monitoring Points 4-1-4-9

For the stress analysis of roadway slopes with increasing width of stepped platforms, in order to study the relationship between the stresses at monitoring points 3-5, 4-6 and monitoring points 4-8, 4-9 of stepped slopes with increasing width of platforms, the comparison can be made by making difference method. The point line plots of peak stress versus input acceleration for monitoring points 3-5, 4-6 and monitoring points 4-8, 4-9 are plotted as shown in Fig. 12(a) and Fig. 12(b), and the difference is made to obtain that with the increase of the platform width, the stresses in the outer corners increase and the stresses in the inner corners decrease.

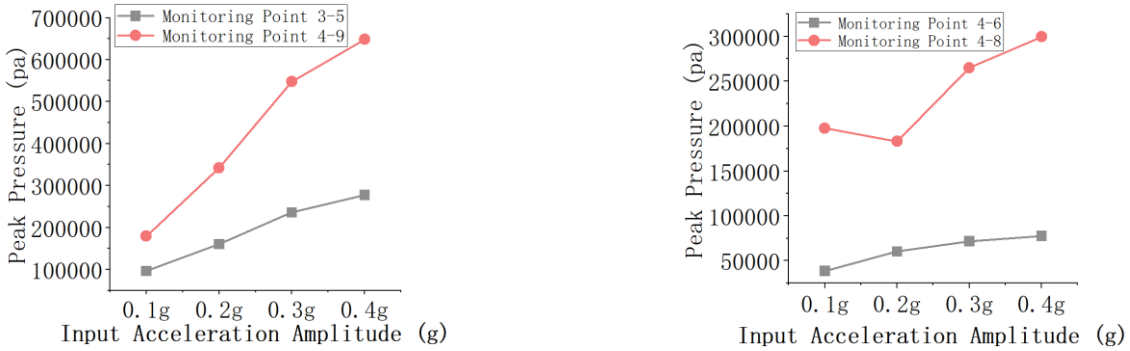

Fig. 12 (a) Monitoring points 3-5 and 4-9 (b) Monitoring points 4-6 and 4-8

4. Conclusions

1) Response acceleration and response displacement exhibit elevation amplification effects.

2) The magnitude of input acceleration directly influences the response acceleration and response displacement.

3) Following seismic wave loading, platform width has a greater impact on the stability of graben slopes compared to slope rate.

4) Slope failure is more likely to occur on the inner side of the bridleway due to concentrated stresses exceeding shear strength.

5) In the case of stepped graben slopes, the outer corner experiences higher acceleration and displacement than the inner corner, while the outer corner stress is lower than the inner corner stress.

6) In step-type platforms with increasing road rift valley slopes, as the platform width increases, the outer angular acceleration decreases and the inner angular acceleration increases. Similarly, the

outer angular displacement decreases, and the inner angular displacement increases. The outer angular stress increases, whereas the inner angular stress decreases.

7) According to the dynamic response law of slopes, study the dynamic damage evolution process of slopes, and provide a theoretical basis for the study of seismic reinforcement measures of slopes.

References

[1] Jinzhong Sun, Saichao Han, Feng Xiong, et al. Analysis of seismic instability probability of slopes[J]. Xinjiang Geology,2020,38(02):262-268.

[2] Qiang Xu, Runqiu Huang. large-scale avalanche-landslide hazard induced by the 5.12 Wenchuan earthquake[J]. Journal of Engineering Geology, 2008, 16 (6) :721-729.

[3] Yongshuang Zhang, Yuliang Cheng, Xin Yao et al. Evolutionary process of earthquake- landslide-mudslide disaster chain formation in Wenchuan, Sichuan [J]. Geological Bulletin, 2013, 32 (12): 1900-1910.

[4] Weiwei Bai, Lei Shi, Fubao WU, et al. Study on dynamic response of multi-stage platform graben slopes under earthquake[J]. Hydropower Generation,2020,46(09):63-68.

[5] Zehua Zhou. Study on dynamic response and time-frequency stability of slopes with penetrating structural face under strong seismic action[D]. Chang'an University,2023.

[6] Jibo Wang. Three-dimensional dynamic response analysis of slope geohazard susceptibility and hazardous slopes in Dalian area[D]. Dalian University of Technology,2023.

[7] Chenyang Ma. Characteristics of dynamic response and stability evaluation of reservoir bank slopes under the action of underwater drilling and blasting[D]. China University of Geosciences, 2022.

[8] Junyu Tian. Numerical simulation study on dynamic response and stability of slopes of base-covered mound under earthquake [D]. Southwest Jiaotong University,2022.

[9] QI Sheng-Wen. Two patterns of dynamic responses of single free surface slopes and their threshold height[J]. Chinese Journal of Geophysics,2006,49(2):518-523.

[10] QI Sheng-Wen, WU Fa-Quan. Study on the regularity of dynamic response for slope [J]. Science in China SeriesE,2003,33(Supp.):28-40.

[11] QI Sheng-wen, WU Fa-quan, LIU Chun-ling,et al.Engineering geology analysis on stability of slope under earthquake[J].Chinese Journal of Rock Mechanics andEngineering,2004,23(16):2792-2797.

[12] Shuaihua Ye, Anping Huang, Guangwen Fang. Dynamic response law and stability analysis of loess multilevel high-fill slopes under horizontal seismic action[J]. Earthquake Defense Technology,2020,15(01):1-10.

[13] Shiyuan Huang, Jian Liu, Zengkai Deng et al. Influence of platform width on slope dynamic response and stability under horizontal ground shaking[J]. China Science and Technology Paper,2015,10(07):839-845.

[14] Sun Ke Yi. Analysis on the influence of slope platform width on slope stability based on slope platform width [J]. Qinghai Transportation Science and Technology, 2017, (06): 75-78.

[15] Hongbing Guan. Application of FLAC3D numerical analysis software in deep foundation pit engineering[J]. Journal of Anyang Institute of Technology,2021,20(02):82-85.